THE RÔLE OF ASYMPTOTIC ANALYSIS IN QUANTIFYING THE PROCESS ZONE IN NOTCHES AND CRACKS

D.A. Hills* and D. Dini

Department of Engineering Science,
University of Oxford, Parks Road, OX1 3PJ, Oxford (U.K.)

Abstract. This paper reviews the quantification of process zones at the roots of notches and cracks, and examines their characterisation by asymptotic solutions. The effect of a local radius at the root of the feature on the validity of the process zone is then considered, and clear guidelines given for what combinations of load and root-radius are acceptable. Finally, a quantitative comparison is made between the solutions for notch roots and crack roots, so that the possibility of treating certain kinds of nearly sharp notches as cracks may be assessed, with a view to deriving crack nucleation predictions.

1. INTRODUCTION

This paper is concerned with the characterisation of the process zone at the roots of cracks and notionally sharp notches, using asymptotic elasticity solutions. The intention is to build up a picture of the nature of the stress state at the apex of these features, using, wherever possible, a single parameter (a generalisation of the stress intensity concept in fracture mechanics). The first step is to establish the nature of the local solution, and to apply it to a range of finite crack and notch problems. This will permit the maximum size of the plastic zone to be found in order for it to be characterised completely by the singular field. We shall then go on to look at a new set of semi-infinite solutions, due to Filippi et al. [1], and which incorporate a radius at the tip of the notch or 'crack'. These solutions, though not exact, are of extremely high fidelity, and permit the effect of a local radius to be found explicitly. Lastly, because the family of asymptotic solutions presented are of the 'variables separable' kind (in polar co-ordinates (r, θ)), and the crack solution is merely a special case of the sharp notch, a clear comparison between cracks and notches is possible. This will then permit the solution for a radiused notch to be matched with that of the nearest crack (in the sense of choosing a crack tip stress intensity factor which allows the crack tip field to resemble the notch field with a given degree of precision). It follows that the process zone at the notch root, which may lead to the formation of a crack, may be thought of as being in some respects 'equivalent' to a crack. Although this has yet to be verified experimentally, it raise questions of whether the threshold stress intensity factor (ΔK_{th}) may be used to predict the go-no-go condition for the *initiation* of a crack. Note that this statement is not, physically, equivalent to short crack growth procedures for assessing the same problem.

2. FUNDAMENTALS OF ASYMPTOTICS

2.1. Sharp Asymptotic Solution

The basic solution needed to characterise the stress state at a sharp corner (whether that corner be a notch apex or a crack tip) is the celebrated Williams solution [2] for the stress state near the apex of a semi-infinite 'wedge', (Fig. 1). This problem is treated fully in postgraduate textbooks such as Barber [3], and, for economy of space, we shall present only an outline of the solution here. A solution is sought for the state of stress in the neighbourhood of the wedge apex, ensuring that the free faces of the wedge are devoid of tractions. A stress function in polar coordinates is chosen, from which the traction components of stress may be found, and the requirement that these vanish on $\theta=\pm\alpha$ leads to the following two pairs of simultaneous linear homogeneous equations:

$$\begin{bmatrix} (1+\lambda)\cos(1-\lambda)\alpha - \cos(1+\lambda)\alpha & 0 \\ (1-\lambda)\sin(1-\lambda)\alpha - \sin(1+\lambda)\alpha & (1+\lambda)\sin(1-\lambda)\alpha - \sin(1+\lambda)\alpha \\ 0 & (1-\lambda)\cos(1-\lambda)\alpha - \cos(1+\lambda)\alpha \end{bmatrix} \begin{bmatrix} A_1 \\ A_3 \\ A_2 \\ A_4 \end{bmatrix} = \begin{bmatrix} 0 \\ 0 \\ 0 \\ 0 \end{bmatrix} \tag{1}$$

*Corresponding author: david.hills@eng.ox.ac.uk, Phone: +441865273119, Fax: +441865273906

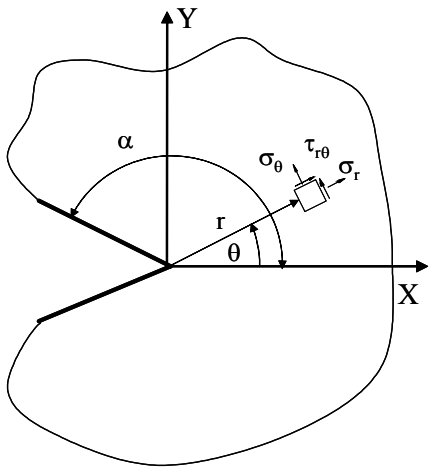


Fig. 1. Wedge problem.

In order for their solution to be unique the determinant of the coefficients must vanish, and this leads to the following pair of characteristic equations:

$$\lambda \sin(2\alpha) \pm \sin(2\lambda\alpha) = 0 \qquad (2)$$

The plus sign relates to symmetric loading and the negative sign to antisymmetric loading. The stress state itself is given by

$$\begin{Bmatrix} \sigma_{\theta\theta} \\ \sigma_{rr} \\ \sigma_{r\theta} \end{Bmatrix} = \begin{bmatrix} -\lambda(\lambda+1)\cos(\lambda+1)\theta & -\lambda(\lambda-1)\cos(\lambda-3)\theta \\ \lambda(\lambda+1)\cos(\lambda+1)\theta & \lambda(\lambda+1)\cos(\lambda-1)\theta \\ \lambda(\lambda+1)\sin(\lambda+1)\theta & \lambda(\lambda-1)\sin(\lambda-1)\theta \end{bmatrix} \begin{bmatrix} A_1 \\ A_3 \end{bmatrix} r^{\lambda-1}, \qquad \textit{symmetric}$$

$$\begin{Bmatrix} \sigma_{\theta\theta} \\ \sigma_{rr} \\ \sigma_{r\theta} \end{Bmatrix} = \begin{bmatrix} -\lambda(\lambda+1)\sin(\lambda+1)\theta & -\lambda(\lambda-3)\sin(\lambda-1)\theta \\ \lambda(\lambda+1)\sin(\lambda+1)\theta & \lambda(\lambda+1)\sin(\lambda-1)\theta \\ -\lambda(\lambda+1)\cos(\lambda+1)\theta & -\lambda(\lambda-1)\cos(\lambda-1)\theta \end{bmatrix} \begin{bmatrix} A_2 \\ A_4 \end{bmatrix} r^{\lambda-1}, \qquad \textit{antisymmetric} \qquad (3)$$

where λ, and hence the ratios A_1/A_3 and A_2/A_4 , are fixed by the notch angle α.

In this paper we shall subsequently restrict our attention to symmetric loading ('mode I loading' in fracture mechanics terminology), and it will be noted that the exponent λ - 1 is negative, giving rise to a singular state of stress, for all re-entrant wedges ($2\alpha > \pi$), i.e. notches. The exponent is most strongly singular when the notch angle in the material, 2α, goes to 2π radians, and the notch becomes, as a special case, a crack.

2.2. Rounded Asymptotic Solution

A very interesting and powerful paper has recently been published by Filippi et al. [1]. In it, a description is given of an approximate solution for the state of stress near the apex of a semi-infinite 'wedge', but having a finite apex radius, ρ, Figure 2(b). It will be appreciated that the solution found must, asymptotically, become the same as that for a sharp wedge when the observation point r/ρ becomes remote from the apex, i.e. this dimensionless ratio becomes large. Similarly, there is a requirement common to the two problems that the traction components of stress must vanish on the straight flanks of the wedge. The additional requirement is that the tractions should also vanish around the radiused apex. Thus Filippi et al. sought a perturbation to the Williams solution which became small when the observation point became remote. It follows that the perturbation must itself be a set of power order terms, with an exponent which is more strongly singular than the underlying wedge solution. In fact a series expansion of this general kind may possibly be used to solve the problem exactly, but in Filippi's solution a single higher order term is employed, and this is used to ensure that the tractions vanish precisely at the notch apex, although they may become finite (if small), at other points around the radiused portion of the surface. The solution has the following form:

$$\sigma_{ij}(r,\theta) = K_I^* r^{\lambda-1}\left[f_{ij}(\theta,\alpha) + g_{i,j}(r,\theta,\alpha)\right] \qquad (4)$$

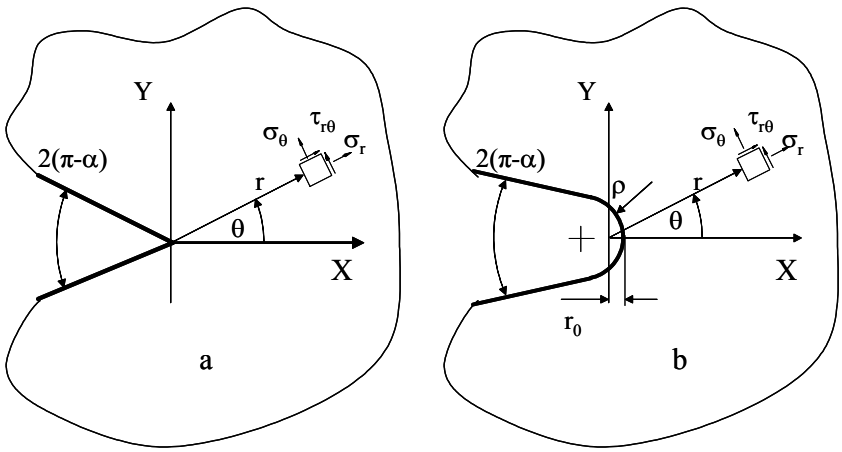


Fig. 2. (a) Semi-infinite sharp notch; (b) Semi-infinite rounded.

The eigenfunctions $f_{ij}(\theta,\alpha)$ can be written as:

$$\begin{Bmatrix} f_{\theta\theta} \\ f_{rr} \\ f_{r\theta} \end{Bmatrix} = \left[\begin{Bmatrix} (1+\lambda)\cos(1-\lambda)\theta \\ (3-\lambda)\cos(1-\lambda)\theta \\ (1-\lambda)\sin(1-\lambda)\theta \end{Bmatrix} + \chi_{b1}(1-\lambda) \begin{Bmatrix} \cos(1+\lambda)\theta \\ -\cos(1+\lambda)\theta \\ \sin(1+\lambda)\theta \end{Bmatrix} \right] \times \frac{1}{(\lambda+1)+\chi_{b1}(1-\lambda)} \tag{5}$$

where

$$\chi_{b_1} = -\frac{\sin[(1-\lambda_1)q\pi/2]}{\sin[(1+\lambda_1)q\pi/2]} \tag{6}$$

with

$$q = \frac{2\alpha}{\pi}. \tag{7}$$

and the functions $g_{i,j}(r,\theta,\alpha)$ are given by:

$$\begin{Bmatrix} g_{\theta\theta} \\ g_{rr} \\ g_{r\theta} \end{Bmatrix} = \left\{ \frac{q\left(\frac{r}{r_0}\right)^{\mu-\lambda}}{4(q\text{-}1)[(\lambda+1)+\chi_{b1}(1-\lambda)]} \right\} \times \left[\chi_{d1} \begin{Bmatrix} [(1+\mu)\cos(1-\mu)\theta] \\ [(3-\mu)\cos(1-\mu)\theta] \\ [(1-\mu)\sin(1-\mu)\theta] \end{Bmatrix} + \chi_{c1} \begin{Bmatrix} \cos(1+\mu)\theta \\ -\cos(1+\mu)\theta \\ \sin(1+\mu)\theta \end{Bmatrix} \right] \tag{8}$$

Here

$$r_0 = \frac{(q\text{-}1)}{q}\rho \tag{9}$$

and

$$\chi_{c1} = \left\{ \left[(1-\mu)^2 - \frac{1}{q}(1+\mu) \right] [3-\lambda-\chi_{b1}(1-\lambda)] - (3-\mu)\varepsilon \right\} \tag{10}$$

$$\chi_{d1} = \left\{ \left[\frac{1-q(1+\mu)}{q} \right] [3-\lambda-\chi_{b1}(1-\lambda)] - \varepsilon \right\} \tag{11}$$

where

$$\varepsilon = (1-\lambda)^2 + \chi_{b1}(1-\lambda^2) - \frac{1}{q}(1+\lambda) - \frac{\chi_{b1}}{q}(1-\lambda), \tag{12}$$

and μ is given by the implicit solution of the following equation:

$$0 = \left\{ \begin{bmatrix} \frac{1-q(1+\mu)}{q} \end{bmatrix} \times [3-\lambda-\chi_{b1}(1-\lambda)] - \varepsilon \right\} (1+\mu)\cos\left[(1-\mu)q\frac{\pi}{2}\right] + \left\{ \begin{bmatrix} (1-\mu)^2 - \frac{1}{q}(1+\mu) \end{bmatrix} \times [3-\lambda-\chi_{b1}(1-\lambda)] - (3-\mu)\varepsilon \right\} (1+\mu)\cos\left[(1+\mu)q\frac{\pi}{2}\right]. \tag{13}$$

3. STRESS INTENSITY SOLUTION AND EFFECT OF TIP RADIUS

In this section we wish to explore the problems which arise when the stress intensity solution is used to characterise a crack or notch tip; this is the central theme of fracture mechanics under conditions of monotonic loading, and fatigue loading.

It is important to recognise the relevance of the singular solution in determining the behaviour of the feature, be it a notch or a crack. The singular solution will encapsulate the behaviour of the stress state at the root of the crack or notch, provided that the process zone falls within certain boundaries. First, the upper bound to the size of the process zone, known as 'small scale yielding' in fracture mechanics nomenclature, is a geometry-dependent characteristic of the solution. It arises because, if the observation point moves too far from the notch root, the presence of the free boundaries of the real (finite) problem no longer exert a negligible influence on the local stress state. When this occurs adjacent to the boundary between the process zone and the elastic hinterland, it means that the process zone itself is no longer surrounded by a region in which the singular solution dominates. This will be considered further in the next section by means of examples – the edge notch or edge crack.

Secondly, a lower bound to the applied load is set by the influence of a finite radius at the tip of the crack or notch. This is easy to appreciate by reference to Figure 2, which depicts a semi-infinite sharp notch and a semi-infinite rounded notch. If the observation point is very remote ($r/\rho \gg 1$) the influence of the local inner radius on the elastic stress state is very small, and the elastic stress field becomes that given by the sharp notch. As the notch root is approached the influence of any radius starts to become more significant, as the second term in equation (4) can no longer be ignored. It follows that, because both the 'perfectly sharp' and 'radiused' solutions may be scaled with the same generalised stress intensity factor, K^*, a direct comparison between the two fields is possible. This has the big advantage that a 'universal' answer to the question 'How big must the process zone be for the tip

radius to be unimportant?' may be answered in a single figure, with the generalised stress intensity factor as a simple normalising parameter.

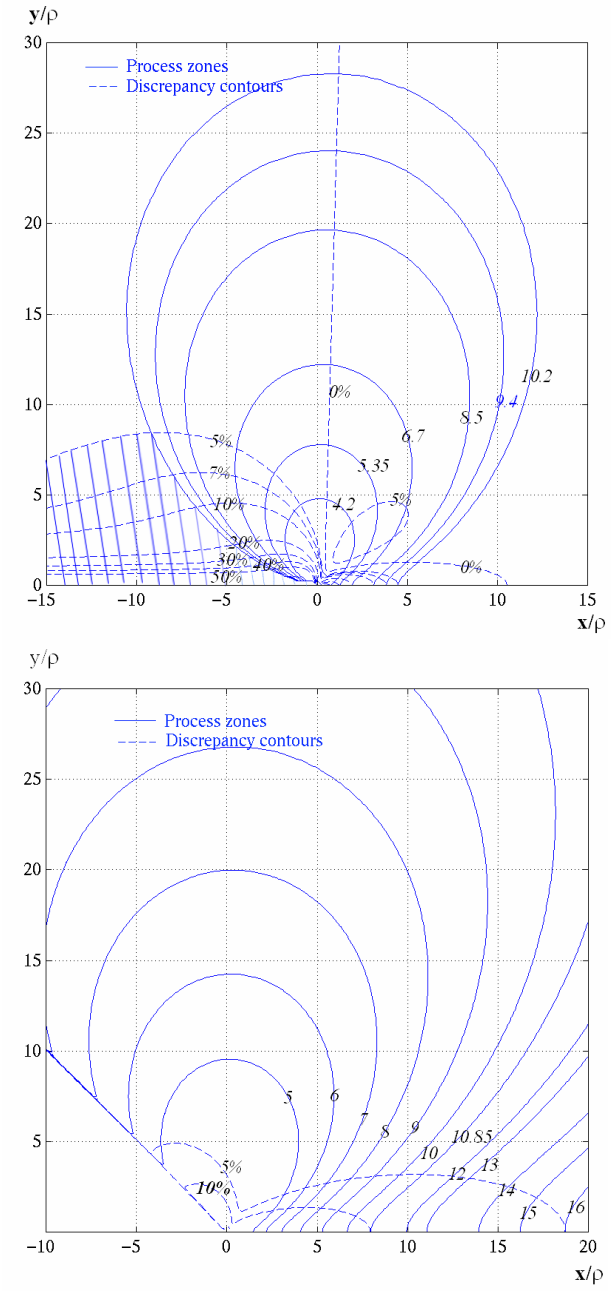


Fig. 3. Discrepancy between solutions for sharp and radiused notch problems together with process zone front locations, for a given normalised stress intensity factor, $K_I^*/(k\rho^{1-\lambda})$: above, 2α = 360 degrees (crack); below, 2α = 270 degrees.

3.1 Lower bound to acceptable load

There is no obvious single measure of the qualities of the stress states that we may use, but, because we shall ultimately be comparing process or plastic zones, it seems natural to use the von Mises plasticity parameter as the measure of stress. Figure 3 includes two sets of contours relating to the notch/crack root, and values are displayed for two useful geoemtries, viz. 2α = 360 degrees (the crack), and 2α = 270 degrees. The first set of contours represents a plot of the fractional mismatch between the sharp and rounded solutions, in the neighbourhood of the root, and using the root radius, ρ, as the non-dimensionalising length scale. The second set of contours represents the physical location of the plastic or process zone front, for various values of the applied load, $K^*/(k\rho^{1-\lambda})$, where k is the yield stress in pure shear.

Thus, by choosing a particular error contour, which is considered an acceptable mismatch between the sharp and blunt solutions, the minimum acceptable load to ensure that the process zone is surrounded by an elastic hinterland defined by the singular solution may be found. Results of these considerations for cracks and notches are displayed in Figure 4, and these provide a very acceptable means of determining the maximum acceptable tip radius. This is the *lower* load bound.

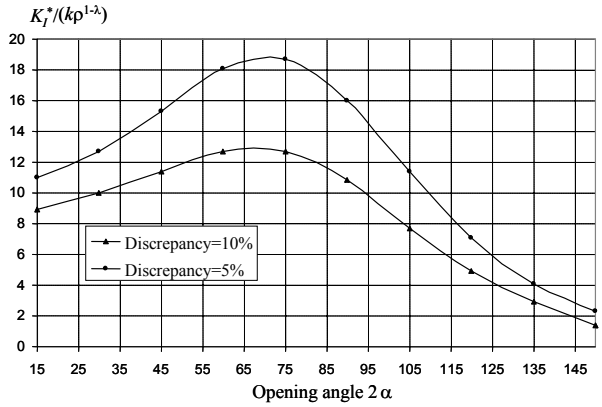


Fig. 4. Comparison between inner and outer solutions (Fig. 2): the minimum normalised stress intensity to achieve characterisation of the process zone to within 5% and 10%.

3.2 Small Scale Yielding Limit

The upper load bound is not quite as 'clean' to define, as the mismatch now is between the singular solution and the full field solution for any feature of this class in a real, finite body, and the rate of divergence of the singular solution from the true solution will clearly depend on the detailed geometry under consideration; the nearer any 'far boundary' the quicker will be the divergence.

As a vehicle to carry out this comparison, we shall use as an example the problem of an edge crack or notch in a semi-finite plane, as shown in Figure 5. As with the 'lower bound' example plots are given for two problems, viz. a 270 degree notch and a 360 degree crack. In this problem the non-dimensionalising length scale is taken as the depth of the feature, *b*, but otherwise the plots drawn are analogous to those found below for the wedge (note that the contours are here plotted in the regions sketched within the margin of the

figures). Again, the two families of contours plotted represent (a) discrepancy, this time between the semi-infinite sharp entity and the finite body (half-plane) with a sharp feature and (b) the location of the plastic front. Again, we wish to ensure that the process zone is fully surrounded by an elastic region dominated by the stress intensity factor. This 'upper bound' to the applied load for a given accuracy is commonly known as the 'small scale yielding' limit in fracture mechanics usage, proposed by Rice [4]. For these edge crack and notch problems, it is summarised in Figure 6.

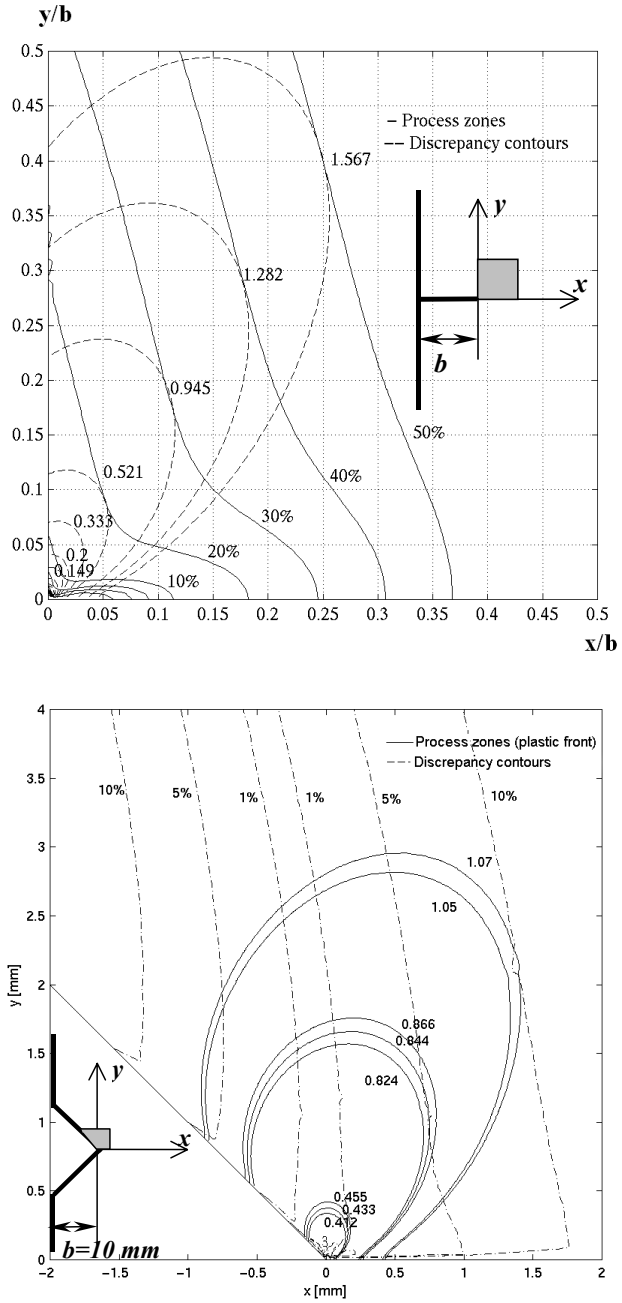


Fig. 5. Discrepancy between finite sharp solution and semi-infinite sharp solution together with process zone front locations, for finite sharp solution, for a given remote load (σ_0/k): above, 2α = 360 degrees (crack); below, 2α = 270 degrees.

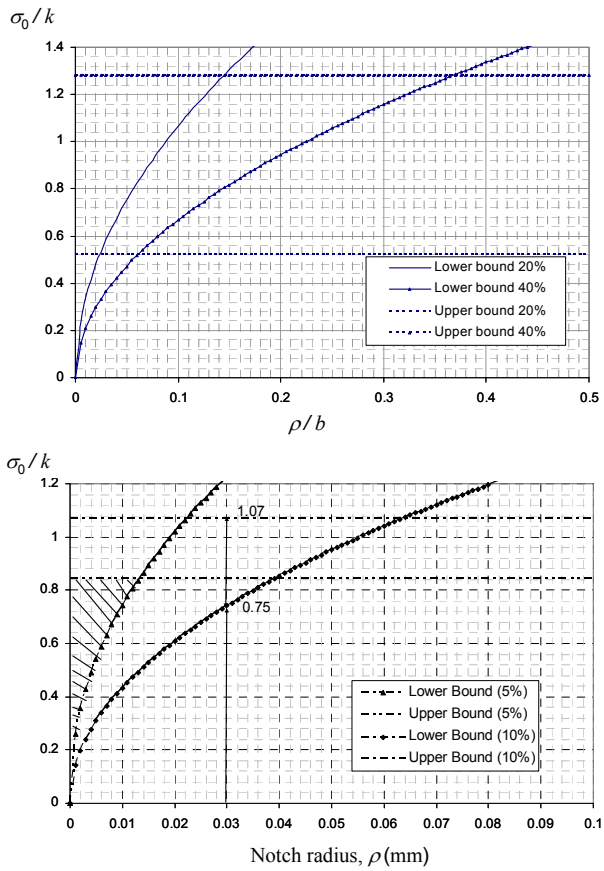


Fig. 6. Range of permissible normalised load (σ_0/k) as a function of notch radius, for the finite problem, to achieve characterisation of the process zone by the singular solution (semi-infinite sharp) to within a given discrepancy: above, 2α = 360 degrees (5%, 7%) and below 2α = 270 degrees. (5%, 10%).

Now, it is possible also to determine the lower load limit from the earlier results in §3.1, employing only the calibration for the generalised stress intensity factor, and the universal plots previously described. Results from this exercise are also included in the summary plot.

3.3 Summary

The results displayed so far may be used in a number of different ways. Perhaps the most direct one is to verify that the load range in a particular case is acceptable for classical singular solutions to apply. Thus, suppose we have an edge crack in a large body. If we decide that we are going to tolerate a maximum discrepancy of 20% between the singular and full field solutions, we see from Figure 3 that the maximum normalised stress intensity tolerable is $K_I / k\sqrt{\rho}$, where k is the yield stress in pure shear. Using the calibration for the stress intensity $K_I / \sigma_0 \sqrt{\pi b} = 1.12$, we see that this corresponds to a maximum applied remote load σ_0/k of 0.521. If we now turn our attention to the lower bound, we see that, to achieve a match of the singular elastic solution for the sharp crack with the

radiused slot to the same accuracy requires that the normalised root radius, ρ/b must be less than about 0.025. The immediate practical application to this result is that, in the case of an artificially formed 'crack', e.g. an EDM formed slot, it gives the maximum end radius which can be tolerated if it is still to behave in a crack-like manner.

Another unexpected point which emerged from this phase of the calculation is the comparative difficulty in securing small scale yielding conditions for the crack compared with the notch. For example, with the same degree of acceptable accuracy cited above, but for a 270 degree notch, the maximum applied remote load may be as great as σ_0/k =1.52.

4. FRAMEWORK OF NOTCH-CRACK COMPARISON

The calculations described above may be extended to permit a careful, quantitative comparison to be made between a 'nearly sharp notch', and a sharp crack. Authors have hinted at or implied such a comparison for a long time [5], but a scientific comparison has proved elusive. The tools described above may be used to answer the question with some precision, and provide the possibility, as yet untested, of using crack *propagation* rules as a means of assessing the possibility of crack *nucleation* from a notch-like feature.

The essence of the comparison stems from the recognition that the asymptotic stress solutions for a perfectly sharp crack and a perfectly sharp notch are of the 'variables separable' kind. The local feature-tip stress fields for each may be written in the form;

$$\sigma_{ij}(r,\theta) = K_I^* r^{\lambda-1}\left[f_{ij}(\theta,\alpha)\right] \qquad (14)$$

and hence matching of the two solutions would require the eigenfunctions $f_{ij,c}(\theta,\pi)$ (crack) and $f_{ij,n}(\theta,\alpha)$ (notch) to be the same, and also for the power order exponent, λ, to be the same. In fact, as will be shown, the spatial distributions of stress in the two problems are remarkably similar for practically arising notch angles (up to say 2α = 282 degrees), and the difference in λ values is of no consequence, as the 'equivalent' crack problem may be scaled, so that, in the region around the process region perimeter, the magnitude of stress in the two problems is the same. First, we will look at the spatial distribution of stress for the crack and notch problem in some detail. As earlier, the measure of stress we shall use is von Mises yield parameter, the second invariant of the stress deviator. We shall assume transverse plane strain conditions, with Poisson's ratio equal to 0.3. It is straightforward to assemble the yield parameter, and this is plotted out in polar form in Figure 7, for the case of the crack and several representative notch angles. These curves may be interpreted physically as being proportional to the polar spread of the plastic region, so that they imply the shape of the process zone. It is quite remarkable how relatively close these lines are; if we start with the crack plot itself as the datum, the lines drift very slightly outwards as the notch angle is decreased to about 2α = 300 degrees; they then move *back*, so that with a notch angle of 2α = 270 degrees the line is almost coincident with the crack problem, and then there is a gradual and systematic drift away as the notch internal angle is increased further. Of course, because as the notch angle increases the physical domain in which the crack lies changes, so the elastic hinterland must also change, but overall the similarity of the responses is very encouraging, and the matching is excellent in the region 'ahead' of the notch tip, where ductility will be exhausted and the crack will form.

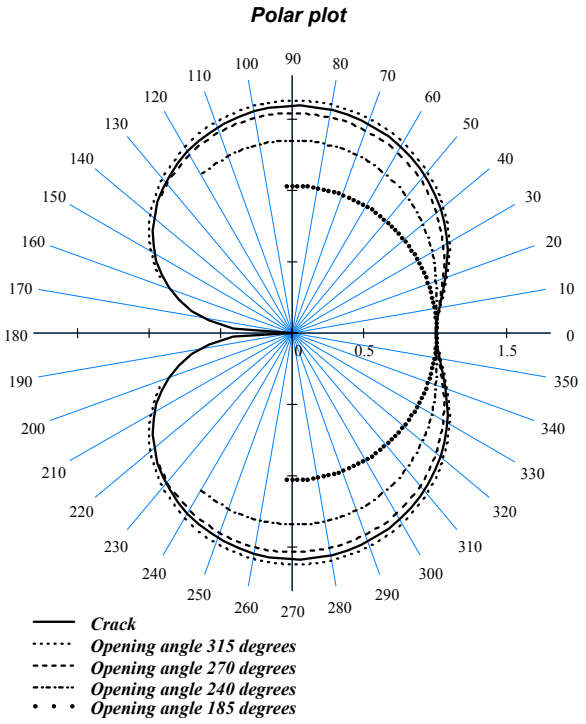


Fig. 7. Measures of the characteristic stress fields of semi-infinite sharp notches and semi-infinite crack: plastic zones polar plot.

We turn, now, to a consideration of the best 'stress intensity factor' to choose for the equivalent crack. This is simply a scaling factor chosen so that the overall size of the process zone in the 'equivalent' crack matches a closely as possible the size of the process zone for the notch. The objective is to deduce the relationship between the stress intensity factors for a sharp notch and that for a crack, such that the process zone in the notch and 'equivalent' crack problems are as nearly matched as possible. In order to do this we need to compare the shape and size of the yield fronts of the two problems ($r_n(\theta)$,$r_c(\theta)$ respectively) by setting $\sqrt{J_2}$ to the yield stress in pure shear, k, for each:

$$\begin{aligned} k^2 &= \left(K_I^* r_n^{\lambda-1}\right) D_n(\theta,\alpha), \qquad \textit{notches} \\ k^2 &= \left(K_I^* r_c^{-1/2}\right) D_c(\theta,\pi), \qquad \textit{crack} \end{aligned} \tag{15}$$

where the subscripts c and n have been added to indicate that we are referring, respectively, to crack or notches and

$$D(\theta,\alpha) = \frac{\sqrt{J_2}}{\left(K_I^* r^{\lambda-1}\right)^2} = \frac{1}{6}\begin{bmatrix} (f_{rr}-f_{\theta\theta})^2 + \\ (f_{\theta\theta}-f_{zz})^2 + \\ (f_{zz}-f_{rr})^2 \end{bmatrix} + f_{r\theta}^2 \tag{16}$$

The size of the yield front is then given by:

$$r_n(\theta,\alpha) = \left(\frac{K_I^*}{k}\right)^{-\frac{1}{\lambda-1}} \left[D_n(\theta,\alpha)\right]^{-\frac{1}{2(\lambda-1)}} \tag{17}$$

$$r_c(\theta,\pi) = \left(\frac{K_I^*}{k}\right)^2 D_c(\theta,\pi)\,. \tag{18}$$

The best match of the process zones will be found by equating the mean values of (18) and (19):

$$\bar{r}_n(\theta,\alpha) = \bar{r}_c(\theta,\pi) \tag{19}$$

where

$$\bar{r}_n(\alpha) = \left(\frac{K_I^*}{k}\right)^{-\frac{1}{\lambda-1}} \bar{D}_n(\alpha) \tag{20}$$

$$\bar{r}_c = \left(\frac{K_I^*}{k}\right)^2 \bar{D}_c\,. \tag{21}$$

and

$$\begin{aligned} \bar{D}_n(\alpha) &= \frac{1}{\pi}\int_0^\pi \left[D_n(\theta,\alpha)\right]^{-\frac{1}{2(\lambda-1)}} d\theta \\ \bar{D}_c &= \frac{1}{\pi}\int_0^\pi D_c(\theta,\pi)\,d\theta \end{aligned} \tag{22}$$

As the solution includes the stress intensity factor, K_I^*, for a finite notch, it is not possible to proceed any further with this calculation without making it specific to the particular geometry in question.

The process just described enables a semi-infinite sharp notch to be compared with an equivalent, or best-fit semi-infinite crack. In the latter case the process zone is fully described by the classical fracture mechanics stress intensity factor, and our assertion is that this should therefore also control the behaviour of the sharp semi-infinite notch. These ideas may be linked to those in the earlier section, delimiting the range of loading and geometry where the semi-infinite elastic solution controls the process zone. We therefore have a viable method for proceeding from a finite stress-raising feature like a blunt notch to the best choice of equivalent crack, and we can also say whether or not this process is feasible for a given geometry

4.1 Application to a rounded edge notch

The example of a radiused edge notch will make the procedure clear. Figure 8 shows a rounded edge notch. We wish to predict whether or notch a crack might nucleate from its root, and the underlying assumption is that there may exist a crack-like plastic process zone there. This is to be characterised by an equivalent crack, whose stress intensity will be found. When once this is known, use of materials data for the threshold of growth should then also be appropriate to determine, for example, the nucleation/no-nucleation condition for the notch.

The analysis will proceed in the following way: first, a finite element (or equivalent numerical procedure) is used to solve for the stress state in the finite actual body. The near-notch stress field is then collocated with solution for a semi-infinite rounded notch. This then isolates the effects of the free boundaries, and puts a limit on the maximum load which the original problem may sustain with 'small scale yielding' conditions being violated. The next step is to compare the semi-infinite radiused notch with the semi-infinite sharp notch of the same angle. We know that these two solutions are coincident remote from the root, and that the concern here is over local divergence, as discussed earlier. Thus, this comparison isolates the effect of the finite radius, and therefore determines the lower bound to the load which may be sustained. Lastly, we move on to a comparison of the semi-infinite notch with the semi-infinite crack, using procedure just described.

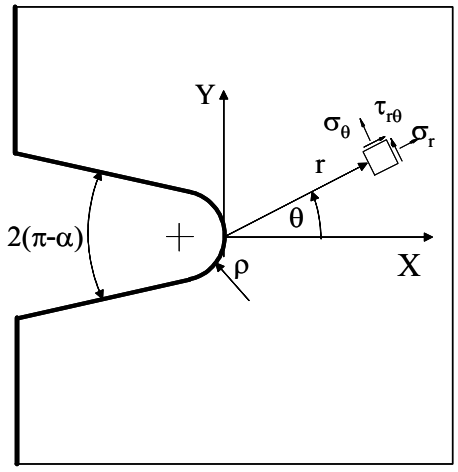


Fig. 8. Edge radiused notch.

The problem to be attacked is shown in Figure 9, which shows a rectangular plate having symmetrically positioned edge notches on the outer edges. This problem was solved using the finite element method.

Two finite element analyses were then carried out using the commercial FEM programme ABAQUS 6.2. The principal dimensions of interest are the notch depth, b, set to 10 mm in each case, and the root radius, ρ, which was set to 0.05 mm in the first model and to 1.0 mm in the second. The models were generated having approximately 30000 elements and 35000 degrees of freedom. The usual precautions in generating an appropriately graded mesh and in ensuring convergence were taken, although, of course, the solution contains no singularities and is therefore well-behaved. The problem of collocating the asymptotic solution differs from those usually encountered in crack and notch problems, insofar as the local field is bounded. Clearly any component of stress in the neighbourhood of the notch root may be used for this purpose, but the $\sigma_{\theta\theta}$ component of stress is finite in this region, and hence provides the most sensitive measure. In this way we find that K_I^*=2.544 and K_I^*=2.68 respectively for ρ/b=0.005 and ρ/b=0.1, where K_I^* is defined by:

$$lim_{r\to 0}\left(\frac{\sigma_{\theta\theta}(r,0)}{r^{\lambda-1}}\right) \qquad (23)$$

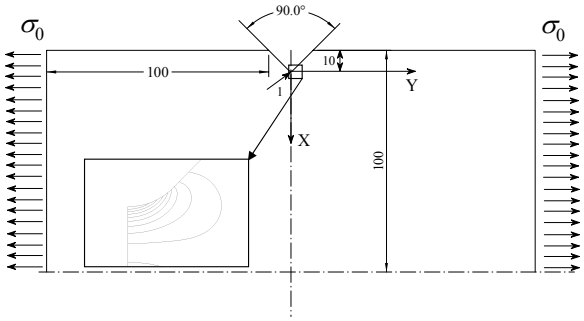


Fig. 9. Finite radiused notch: details of the geometry and shape of the plastic fronts at the notch tip neighbourhood.

Plots of the matching $\sigma_{\theta\theta}$ components along the notch bisector are shown in Fig. 10a. Fig. 10b shows contours of the discrepancy in the elastic states implied by the two solutions, using, this time, the $\sigma_{\theta\theta}$ stress component already used to collocate the solution. As expected, the two solutions are almost identical in the neighbourhood of the notch tip but diverge very quickly due to both the presence of the boundary in the finite model and some small approximation in the solution provided by Filippi et al. [1].

Once the generalised stress intensity factor has been found, it is possible to do two things; first, the region in which the semi-infinite rounded notch and the finite rounded notch solutions match may be found. This sets, in practice, the *maximum* load which may be sustained such that the process zone form is characterised by the semi-infinite radiused solution, and the effect of the free boundaries is small. In order to find this a comparison between the semi-infinite and finite radiused solutions in terms of process zones is needed. As an example, Fig. 11 shows two sets of contours displaying the plastic fronts for semi-infinite and finite radiused problems in the case of ρ/b=0.1. Secondly, we can proceed immediately to determine the *minimum* load which must be applied for the radiused notch to behave like a sharp notch. To do this we consider the solutions to the semi-infinite sharp and radiused problems, which are universal in nature, and independent of the finite problem under consideration. The algebra relating to these two problems has already been considered in detail, and is encapsulated in equations (14) and (4). The principal difference between these solutions is the presence of the functions $g_{ij}(r,\theta,\alpha)$in the latter. Fig. 3b displays the mismatch between these two problems, leaving the generalised stress intensity factor as the intrinsic scaling quantity, and for the specific notch angle 2α=270°.

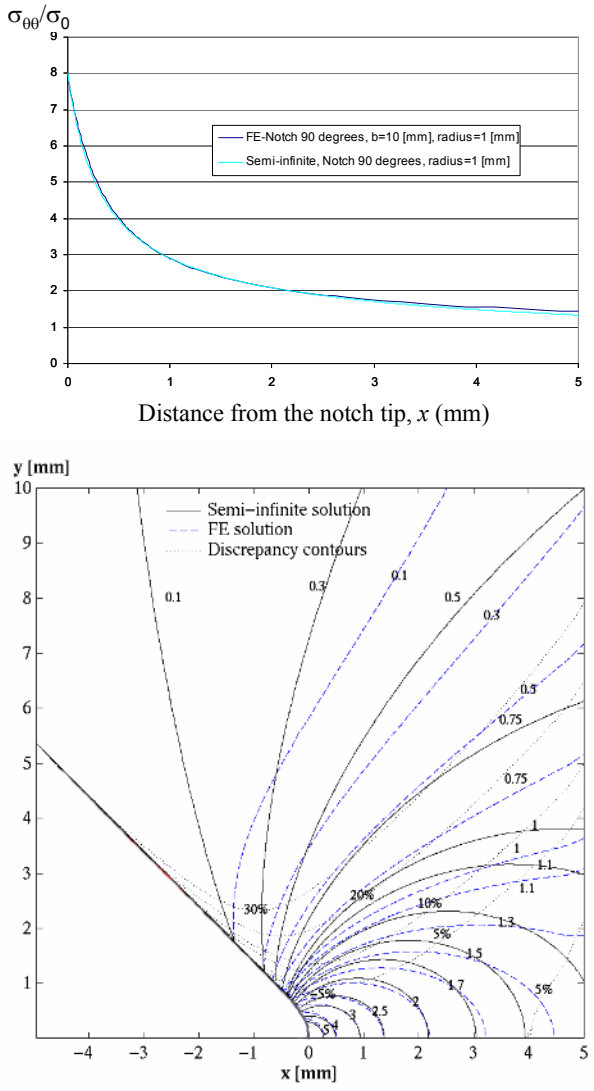


Fig. 10. Deduction of the generalised stress intensity factor for the radiused edge notches and comparison between the FE and calibrated analytical solution for the opening stress component both along the notch bisector for ρ=1, K_I^*=2.68 (above) and at the notch tip for ρ=1 (below).

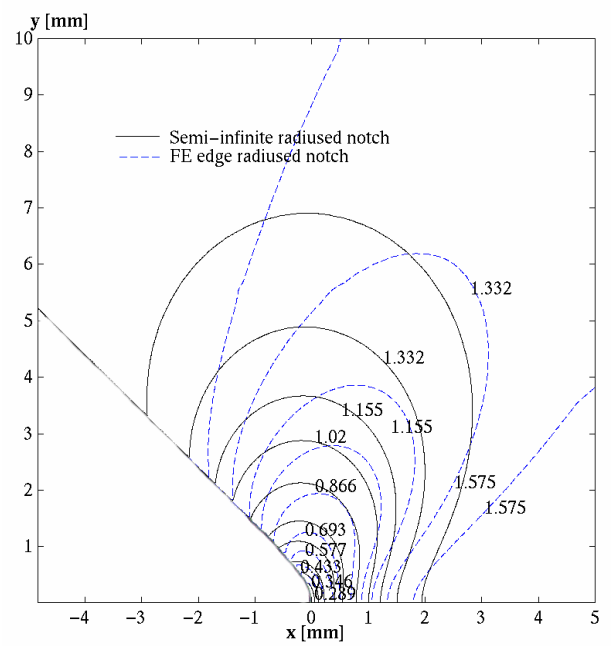


Fig. 11. Plastic front contours for semi-infinite and finite radiused notch *(ρ=1)*.

We will now apply this result to the specific problem just studied, by substituting the calibration values found for the generalised stress intensity factors. This shows that, for a maximum tolerable discrepancy of 10%, the load must be at least σ_0/k=0.834 for ρ/b=0.005 and σ_0/k=4.05 for ρ/b=0.1, whereas for a tolerable discrepancy of 20%, the load must be at least σ_0/k =0.531 for ρ/b=0.005 and σ_0/k =2.57 for ρ/b=0.1. The last phase of the calculation is to compare the semi-infinite crack with the semi-infinite sharp notch problem but this has already been done, above, in relation to the sharp finite notch. As shown in Fig. 7, comparisons between the eigenfunctions of the semi-infinite crack and semi-infinite sharp notches show that, up to and included angle of 2α=270°, the state of stress surrounding the tip of the defect and the relative plastic zones are comparable and, hence, the same kind of mismatch obtained between semi-infinite sharp notches and radiused notches is expected to be held for semi-infinite crack and radiused notches.

5. CONCLUSION

In this paper we have attempted to introduce the idea of using nested asymptotic solutions to quantify the effect of notch root or crack root rounding on the local stress state, and hence process zone. This has been made possible by the recent publication of near-exact analytical solutions for these geoemtries. A major advantage of this technique is that the scaling between the inner and outer asymptotes is provided by the generalised stress intensity factor, so that completely general comparisons may be carried outer, without recourse to solving a finite-geometry problem. The last enters the solution only insofar as it determines the generalised stress intensity factor. We have gone on to show how, for both notches and cracks, the comparison of the inner and outer asymptotes delimits the lower acceptable load. From there we have gone on to make a study of the stress fields ahead of sharp notches and cracks, and this makes it possible to define meaningfully an ‘equivalent crack’.

The set of tools described have different possible applications. For example, if we are forming a ‘crack’ by mechanical means, we can specify the maximum tolerable root radius for the feature truly to appear crack-like, for a given load. The same notion can be applied directly to nearly sharp notches.

We can view the process in a completely different way: we can examine a stress raising notch in a body and ask if it is possible for it to be considered ‘sharp’, and, if so, if it could be treated as a crack. Thus, we start off with a finite, concentrated stress state, and ask if a large process zone would be sufficiently sharp-notch-like, or even crack-like. These ideas set lower bounds to the applied load. The presence of other boundaries set upper bounds and there will, of course, be cases when the upper bound to the acceptable load is lower than the acceptable lower bound. In these cases the concept of an equivalent ‘sharp’ feature in a finite body cannot be sustained, and the process breaks down.

REFERENCES

[1] Filippi, S., Lazzarin, P., and Tovo, R., 2002. Development of some explicit formulas useful to describe elastic stress fields ahead of notches in plates. *International Journal of Solids and Structures*, 39, 4543-4565.

[2] Williams, M.L., 1952. Stress singularities resulting from various boundary conditions in angular corners of plates in tension. *Journal of Applied Mechanics,* 19, 526–528.

[3] Barber, J. R., 1992. *Elasticity*, Kluwer Academic Publishers, Dordrecht, The Netherlands.

[4] Rice, J.R., 1974. Limitations to the small scale yielding approximation for crack tip plasticity, Journal of the Mechanics and Physics of Solids, 22, 17-26.

[5] Smith, R.A. and Miller, K.J., 1978. Prediction of fatigue regimes in notched components, *International Journal of Mechanical Sciences*, 20, 201-206.